Diabetic impairments in NO-mediated endothelial progenitor cell mobilization and homing are reversed by hyperoxia and SDF-1α

Katherine A. Gallagher,[1] Zhao-Jun Liu,[1] Min Xiao,[1] Haiying Chen,[1] Lee J. Goldstein,[1] Donald G. Buerk,[2] April Nedeau,[1] Stephen R. Thom,[3] and Omaida C. Velazquez[1]

[1]Department of Surgery, University of Pennsylvania Medical Center, Philadelphia, Pennsylvania, USA. [2]Departments of Physiology and Bioengineering, University of Pennsylvania School of Medicine, Philadelphia, Pennsylvania, USA. [3]Department of Emergency Medicine, Institute for Environmental Medicine, University of Pennsylvania Medical Center, Philadelphia, Pennsylvania, USA.

Endothelial progenitor cells (EPCs) are essential in vasculogenesis and wound healing, but their circulating and wound level numbers are decreased in diabetes. This study aimed to determine mechanisms responsible for the diabetic defect in circulating and wound EPCs. Since mobilization of BM EPCs occurs via eNOS activation, we hypothesized that eNOS activation is impaired in diabetes, which results in reduced EPC mobilization. Since hyperoxia activates NOS in other tissues, we investigated whether hyperoxia restores EPC mobilization in diabetic mice through BM NOS activation. Additionally, we studied the hypothesis that impaired EPC homing in diabetes is due to decreased wound level stromal cell–derived factor–1α (SDF-1α), a chemokine that mediates EPC recruitment in ischemia. Diabetic mice showed impaired phosphorylation of BM eNOS, decreased circulating EPCs, and diminished SDF-1α expression in cutaneous wounds. Hyperoxia increased BM NO and circulating EPCs, effects inhibited by the NOS inhibitor N-nitro-L-arginine-methyl ester. Administration of SDF-1α into wounds reversed the EPC homing impairment and, with hyperoxia, synergistically enhanced EPC mobilization, homing, and wound healing. Thus, hyperoxia reversed the diabetic defect in EPC mobilization, and SDF-1α reversed the diabetic defect in EPC homing. The targets identified, which we believe to be novel, can significantly advance the field of diabetic wound healing.

Introduction

Impaired wound healing is a major clinical problem in patients with diabetes and is the leading cause of lower extremity amputation (1). Current therapies have a limited success rate and fall short in addressing the microvascular pathology present in diabetics (2, 3). Poor healing of diabetic wounds is characterized by impaired angiogenesis and vasculogenesis. Vasculogenesis involves the growth of neovessels from BM-derived progenitor cells and contributes to the process of postnatal neovascularization and wound healing (4–6). The BM-derived endothelial progenitor cell (EPC) is a key cell involved in vasculogenesis and homes to peripheral tissue in response to ischemia (7, 8). Previous studies have begun to elucidate the mechanisms responsible for the mobilization of EPCs into circulation and their recruitment into areas of peripheral tissue ischemia; however, it remains unknown why the main physiologic stimulus for EPC mobilization and recruitment (i.e., ischemia) fails to induce therapeutic EPC-mediated neovascularization and healing in wounds of diabetic hosts.

It has been previously reported that EPCs are mobilized from BM into circulation, home to sites of ischemia, undergo in situ differentiation, and ultimately participate in the formation of new blood vessels (8–10). This EPC mobilization cascade starts with peripheral hypoxia-induced tissue release of VEGF-A and subsequent activation of BM stromal NOS, resulting in increased BM NO levels (11, 12). In this process, eNOS is essential in the BM microenvironment, and increases in BM NO levels result in the mobilization of EPCs from BM niches to circulation, ultimately allowing for their participation in tissue-level vasculogenesis and wound healing (13, 14). At the tissue level, EPC recruitment depends on ischemia-induced upregulation of stromal cell–derived factor–1α (SDF-1α) (15). Impairments in eNOS function have been reported with hyperglycemia, insulin resistance, and in peripheral tissue from diabetic patients (16–20), however, there are no reported prior studies of eNOS function in BM cells in diabetes. In addition, there are no previous studies examining the effects of diabetes on the expression of SDF-1α within cutaneous wounds.

While hypoxia-induced signals for EPC mobilization have been reported, the effect of therapeutic hyperoxia on this pathway is unknown. Induction of hyperoxia, via hyperbaric oxygen therapy (HBO), has been shown to increase NO levels in perivascular tissues via stimulation of NOS (21, 22). Because the generation of NO results in EPC release from the BM and HBO has been shown to stimulate NO production in other tissues, we examined the effect of hyperoxia on activation of NOS in BM. We recently determined that HBO increases BM NO levels via a NOS-mediated mechanism in nondiabetic wild-type mice (23). The effects of diabetes on this hyperoxia-mediated NO increase in the BM has not been previously studied. At a clinical level, current FDA-approved hyperoxia

Nonstandard abbreviations used: CXCR4, CXC chemokine receptor 4; EPC, endothelial progenitor cell; HBO, hyperbaric oxygen therapy; L-NAME, N-nitro-L-arginine-methyl ester; SDF-1α, stromal cell–derived factor–1α; STZ, streptozocin.

Conflict of interest: The authors have declared that no conflict of interest exists.

Citation for this article: *J. Clin. Invest.* **117**:1249–1259 (2007). doi:10.1172/JCI29710.

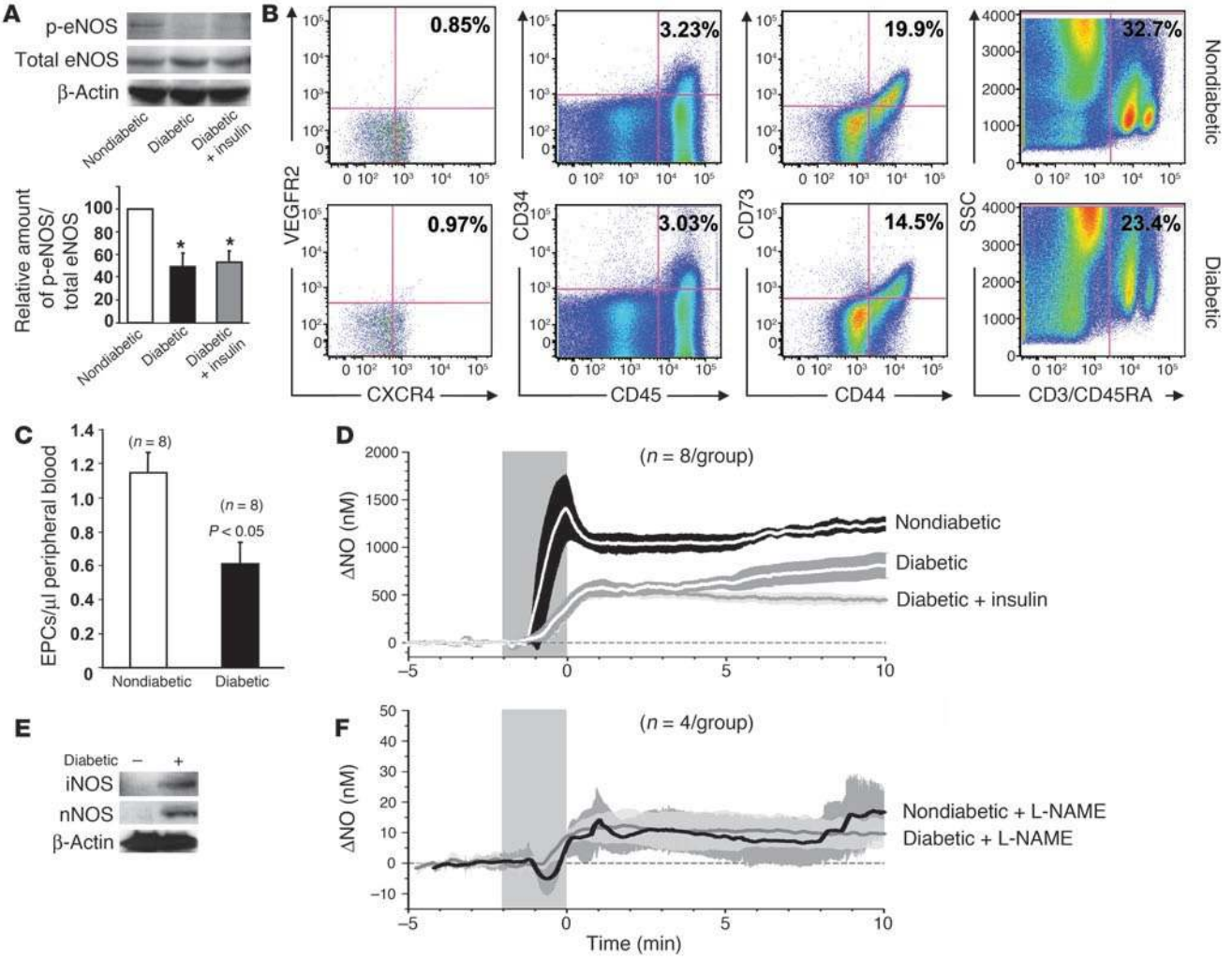

Figure 1

Impaired phosphorylation of BM eNOS with attenuation of HBO-induced NO levels results in decreased circulating EPCs in diabetic mice. (**A**) Representative Western blot analysis for BM eNOS. Diabetic mice demonstrated decreased phosphorylated eNOS compared with nondiabetic controls. Insulin failed to restore impaired eNOS phosphorylation. Quantification of phospho-eNOS (p-eNOS). Results are based on 4 experiments and show the amount of phospho-eNOS relative to total eNOS and β-actin. Nondiabetic controls are used as the standard (value set at 100). *$P < 0.01$. (**B**) Changes in cell composition in BM of diabetic mice. EPC (VEGFR2/CXCR4) and HSC (CD34/CD45) populations are unchanged, while mesenchymal stromal (CD73/CD44) and inflammatory cell (SSC/CD3/CD45RA) populations are slightly decreased in diabetic mice compared with nondiabetic mice. Percentages indicate positive cells in total BM cells counted. (**C**) Quantification of the number of Tie2$^+$/VEGFR2$^+$ EPCs/μl of peripheral blood in Tie2-GFP mice by flow cytometry at 7 days following STZ treatment. A substantial reduction in circulating EPCs was found in diabetic compared with nondiabetic mice. (**D** and **E**) NO production in the BM cavity of diabetic and nondiabetic mice during 10 minutes of HBO treatment. Baseline NO levels were obtained 5 minutes prior to onset of pressurization at 100% O_2 (gray bar). Solid lines represent mean values, with surrounding gray or black shading representing SEM. (**D**) Hyperoxia increases BM NO levels significantly, but the NO response is attenuated in diabetic mice compared with nondiabetic animals ($P < 0.05$). Insulin did not reverse the impairment of NO production. (**E**) Total iNOS and nNOS proteins were upregulated in diabetic mice. –, nondiabetic mice; +, diabetic mice. (**F**) Complete inhibition of BM NO production in diabetic and nondiabetic mice undergoing HBO treatment after pretreatment with L-NAME.

(i.e., HBO) protocols in diabetic patients have demonstrated inconsistent results in the wound healing response (24–26), underlining the need to elucidate the mechanisms responsible for the therapeutic effects of HBO.

In this study, we hypothesized that diabetes results in impaired BM eNOS activation and hence reduced mobilization of EPCs from BM into circulation. We then tested whether hyperoxia may specifically enhance BM NOS activity, resulting in increased or restored systemic EPC mobilization in diabetic mice. Specifically, we determined whether a diabetes-associated defect in the production of biologically active eNOS, and thus EPC mobilization, can be reversed by hyperoxia.

We determined that, while hyperoxia increases the mobilization of EPCs into circulation, these cells do not effectively home to diabetic cutaneous wounds. In cutaneous wounds, SDF-1α may function as a homeostatic regulator of tissue remodeling (27). Since cutaneous wounds in diabetic hosts are known to show chronic inflammation and disorganized tissue repair that signifi-

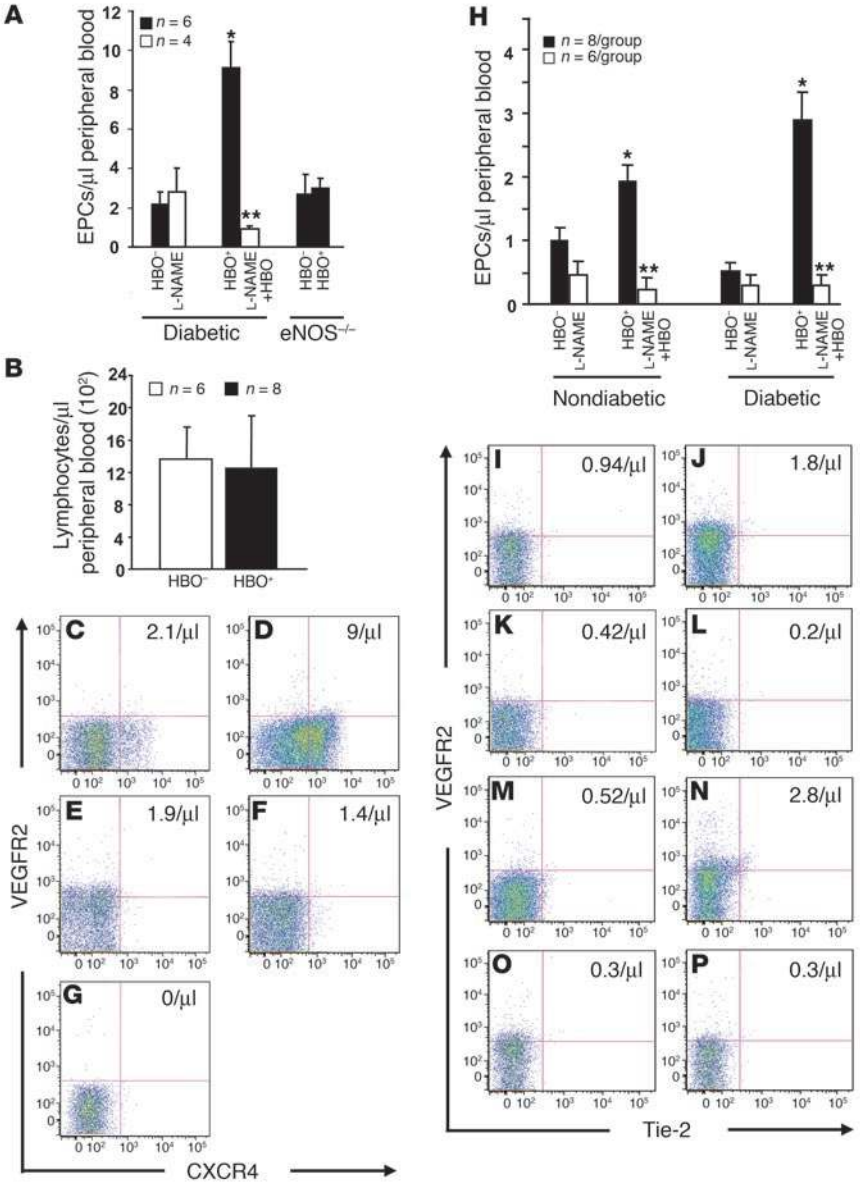

Figure 2
NO-dependent EPC, not lymphocyte, mobilization is enhanced by hyperoxia. Flow cytometry quantification of circulating peripheral blood EPCs (CXCR4⁺/VEGFR2⁺) (**A**) and lymphocytes (**B**) in diabetic FVB and eNOS$^{-/-}$ mice and peripheral blood EPCs (Tie2⁺/VEGFR2⁺) in Tie2-GFP (**H**) mice. Data are based on 6 (**A** and **B**) and 12 (**H**) experiments. Mice were treated with or without HBO (HBO⁺ and HBO⁻, respectively) or with L-NAME ± HBO. *$P < 0.05$; **$P < 0.005$. (**C**–**G** and **I**–**P**) HBO significantly increased circulating EPCs, while L-NAME inhibited this effect. Representative dot plots with number of circulating EPCs in peripheral blood of diabetic FVB (**C**–**G**) and nondiabetic (**I**–**L**) and diabetic (**M**–**P**) Tie2-GFP mice are shown. (**C**, **I**, and **M**) HBO⁻, (**D**, **J**, and **N**) HBO⁺, (**E**, **K**, and **O**) L-NAME, and (**F**, **L**, and **P**) L-NAME+HBO. (**G**) Isotype control (VEGFR2/CXCR4).

cantly delay healing, we hypothesized that expression of SDF-1α within diabetic peripheral wound tissue is significantly decreased, accounting for the diabetic defect in EPC homing. To examine this question, we studied the expression of the EPC-homing chemokine SDF-1α and the cell source for SDF-1α production in wounds of diabetic mice. We then tested the hypothesis that exogenous administration of SDF-1α to wounds of diabetic mice increases wound-level EPC recruitment. Furthermore, we investigated the use of hyperoxia to increase EPC mobilization combined with SDF-1α to promote EPC homing to peripheral tissue in order to determine the therapeutic potential for synergistic enhancement of diabetic wound healing.

Results

Impaired phosphorylation of BM eNOS in diabetic mice. eNOS is essential for EPC mobilization from the BM into circulation (13). In diabetic patients, circulating EPCs are decreased in both number and function, and so we hypothesized that BM eNOS activation is impaired in diabetes (28–30). To examine this question, BM was isolated from streptozocin-induced (STZ-induced) diabetic and nondiabetic mice and analyzed via Western blot for levels of total and phosphorylated eNOS protein. Although no changes in the amount of total eNOS protein were observed, the levels of biologically active phosphorylated eNOS protein were decreased in diabetic mice as compared with nondiabetic controls (Figure 1A). To investigate whether the decreased eNOS activity might reflect a change in cellular composition within BM of diabetic mice, we studied the constitution of EPCs, stromal cells, HSCs, and lymphocytes in the BM of STZ-induced diabetic versus nondiabetic mice. The EPC and HSC populations remained constant while the mesenchymal stromal cell and lymphocyte populations demonstrated a slight decrease (by approximately 27% and 26%, respectively) in diabetic compared with nondiabetic mice (Figure 1B). Thus, it is possible that diabetes-induced changes in mesenchymal stromal cell and lymphocyte populations in the BM might be responsible for the observed downregulation of BM eNOS activation.

Circulating EPCs are decreased in diabetic mice. Given the central role of eNOS on EPC mobilization and our results demonstrating impaired eNOS phosphorylation in diabetic BM, we tested the hypothesis that circulating EPCs are decreased in diabetic mice. Our findings demonstrate that diabetic mice have an approximately 50% reduction in circulating EPCs as compared with nondiabetic controls (Figure 1C). Hence, impairment in the phosphorylation of eNOS to its biologically active form likely results in depressed mobilization of EPCs from BM into peripheral circulation.

Hyperoxia-induced stimulation of BM NO production is attenuated in diabetic mice. Physiologically, the NO-mediated EPC release into circulation occurs in response to tissue-level hypoxia (6), although this compensatory response is inadequate in the setting of diabetes and results in severe defects in neovascularization and wound healing. Interestingly, we have determined that hyperoxia is a non-

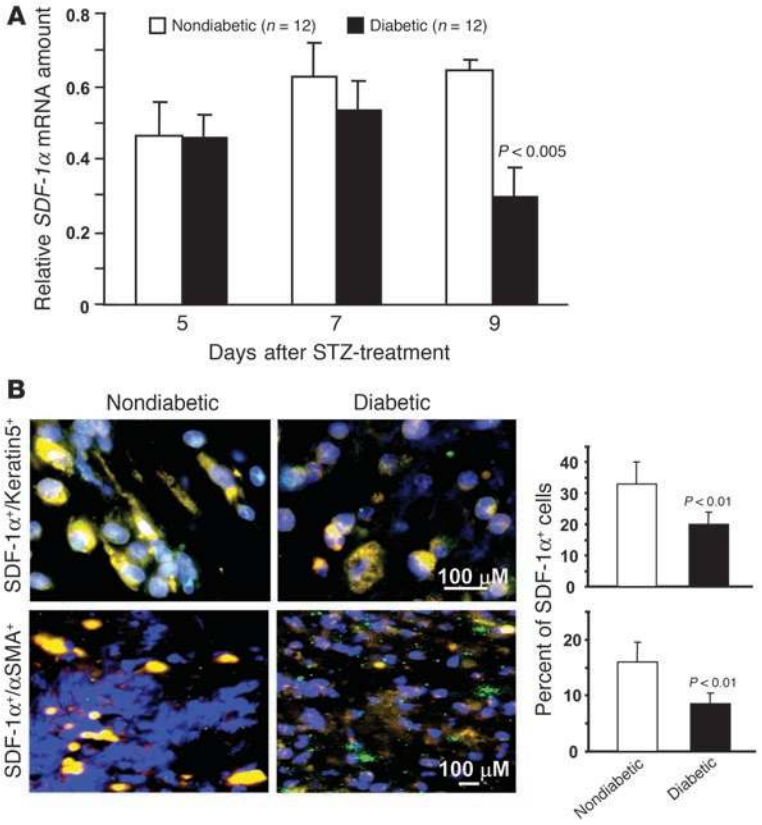

Figure 3
Decreased SDF-1α expression in peripheral wounds of diabetic mice. (**A**) Quantitative detection of the *SDF-1*α mRNA at various time points following STZ treatment in wound tissue of diabetic and nondiabetic mice by real-time RT-PCR. *SDF-1*α mRNA decreased significantly at day 9. Data are based on 3 experiments. (**B**) Left: Epithelial cells and myofibroblasts are impaired in the production of SDF-1α in the wound tissues. Double staining (yellow) of SDF-1α (red) and cell type–specific marker (green) demonstrated a downregulated expression of SDF-1α in epithelial cells and myofibroblasts in diabetic wounds. Right: Percentage of double-positive cells per field. Data are derived from 10 sections of 3 individual experiments.

physiologic stimulus that increases EPC mobilization via a similar NO-mediated mechanism (23). Therefore, we sought to utilize HBO as a tool to augment EPC release into circulation and further study both EPC mobilization and wound-homing mechanisms in the presence of diabetes. We aimed to determine whether hyperoxia stimulates NO production in the BM of diabetic mice via a NOS-mediated pathway and whether this pathway is impaired in diabetes. To test this hypothesis, we inserted Nafion polymer–coated NO microsensors into the femur BM space of both STZ-induced diabetic and nondiabetic mice to measure real-time NO levels within the BM prior to and during HBO-induced hyperoxia. As predicted, diabetic mice demonstrated a significantly attenuated rise in BM NO in response to hyperoxia (Figure 1D). Despite this attenuated response, significant increases from baseline were still observed in BM NO levels in response to hyperoxia in the diabetic mice. Specifically, diabetic mice demonstrated an 800-fold increase in BM NO levels during hyperoxic therapy, as compared with a 1,200-fold NO rise in nondiabetic controls. We speculated that this was likely due to a compensatory effect from other NOS isoforms, and therefore we examined the level of both iNOS and nNOS in diabetic mice. As anticipated, the expression of both total iNOS and nNOS protein was upregulated in diabetic mice (Figure 1E). However, we did not observe any changes in the phosphorylation of these NOS isoforms (data not shown). These data suggest that upregulated NOS isoforms require additional stimuli, such as hyperoxia, to be activated in diabetic mice. Consistent with this, hyperoxia-induced increases in NO production were completely inhibited in both the diabetic mice and the nondiabetic controls by pretreatment with N-nitro-L-arginine-methyl ester (L-NAME), a nonspecific NOS inhibitor that inhibits all 3 isoforms of the NOS enzyme (Figure 1F). Hyperbaric normoxic pressurized and hyperoxic nonpressurized control conditions were also studied and demonstrated no increase in BM NO production (data not shown), confirming that hyperoxia is the key stimulus for the BM NOS activation.

Increases in BM NO induced by hyperoxia stimulate mobilization of BM EPCs into peripheral circulation in diabetic mice. Physiologically, increased levels of BM NO result in activation of MMP-9 and conversion of kit ligand to its soluble form, ultimately generating EPC release into circulation (11, 31). To study the effects of the hyperoxia-induced rise in NO levels in the BM cavity on mobilization of EPCs into circulation, peripheral blood from diabetic mice was analyzed for EPCs using flow cytometry. We determined whether hyperoxia, induced by HBO, increases the number of circulating EPCs in the peripheral blood of diabetic mice. Specifically, we examined peripheral blood of diabetic mice 18 hours after a single HBO treatment. After excluding dead DAPI$^+$-labeled cells, candidate lymphocytes, identified by their typical appearance on forward and side scatter plots, were gated and CD45$^+$/CD3$^+$ cell populations excluded (data not shown). Although EPC markers in humans are well established, the markers that are present on murine EPCs have yet to be precisely defined. Therefore, we used several marker combinations to quantitate circulating EPCs. In independently repeated experiments, EPCs were identified as cells double labeled with either Tie2 and VEGFR2 (32, 33) or (CXC chemokine receptor 4) CXCR4 and VEGFR2 (8, 15, 34). Following treatment with hyperoxia, diabetic mice demonstrate a significant 5-fold increase in circulating CXCR4$^+$/VEGFR2$^+$ EPCs and Tie2$^+$/VEGFR2$^+$ EPCs (Figure 2). Nondiabetic mice treated with HBO showed a similar increase in circulating EPCs, however, the effects of hyperoxia on EPC mobilization were less pronounced as a result of the higher baseline circulating EPC level in the nondiabetic animals. Unlike EPCs, the numbers of circulating lymphocytes were unchanged before and after HBO treatment (Figure 2B), indicating that hyperoxia does not affect lymphocyte mobilization in diabetic mice. In order to specifically determine whether the hyperoxia-induced EPC mobilization is the result of NOS activation, a group of mice were treated with L-NAME prior to HBO treatment. No increase in EPC mobilization following HBO treatment was observed in any of the L-NAME–pretreated animals. In addition, the effect of HBO on EPC mobilization in eNOS$^{-/-}$ mice was examined. No significant changes in EPC mobilization after HBO treatment were observed (Figure 2A), indicating that eNOS is essential

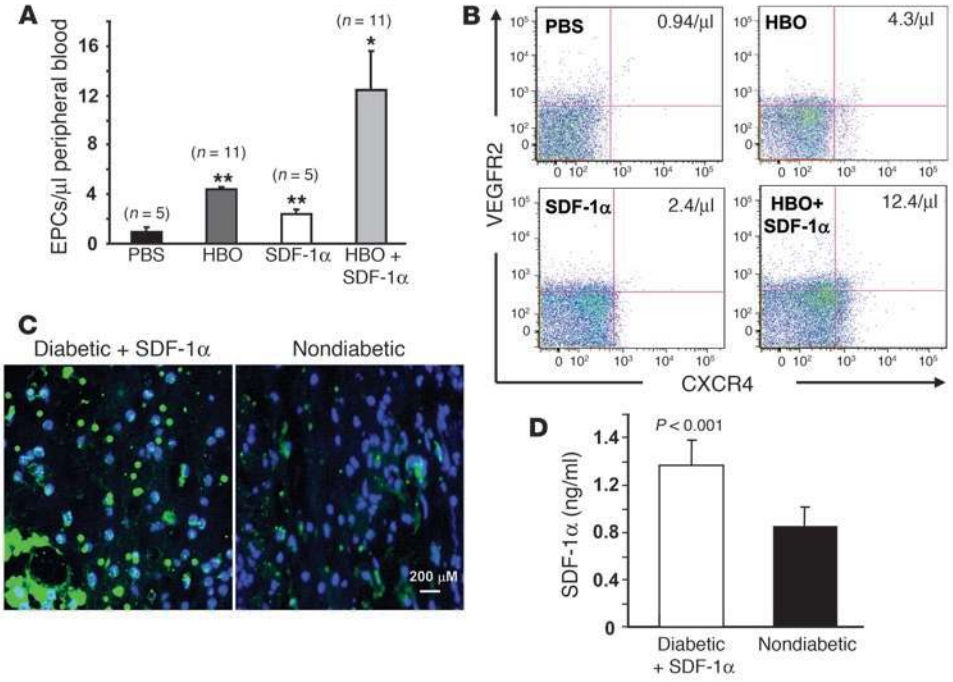

Figure 4

Synergistic enhancement of EPC mobilization by HBO and SDF-1α in a murine diabetic model. (**A**) Diabetic mice were divided into 4 groups that received daily wound injections with either SDF-1α or PBS. Half of the mice also received daily HBO. Forty-eight hours after wounding, peripheral blood was analyzed by flow cytometry. Quantification of EPCs was performed for each group. Data are based on 10 experiments. SDF-1α+HBO–treated mice had a significant increase in circulating EPCs compared with other groups (*$P < 0.05$). SDF-1α- and PBS+HBO–treated groups demonstrated a statistically significant increase as compared with the PBS-treated group (**$P < 0.05$). (**B**) Representative dot plots are shown, with number of peripheral blood EPCs noted in each of the $CXCR4^+/VEGFR2^+$ quadrants. (**C**) Immunostaining demonstrated a supraphysiologic level of SDF-1α in diabetic wounds after SDF-1α injection compared with nondiabetic wounds. (**D**) Local administration of SDF-1α results in supraphysiologic systemic peripheral blood SDF-1α level above that present in nondiabetic mice. ELISA demonstrated an increased systemic SDF-1α concentration 2 hours following local wound injection with SDF-1α.

for hyperoxia-induced EPC mobilization. Consistent with this, BM NO production in $eNOS^{-/-}$ mice was significantly reduced (by approximately 40%; data not shown), although not completely obliterated (likely due to the partial compensatory effect of other NOS isoforms, such as iNOS and nNOS), during HBO therapy. Overall, these data demonstrate that hyperoxia, via an eNOS/NO-mediated mechanism, increases mobilization of EPCs from BM into circulation and reverses the preexisting circulating EPC deficit in diabetes, thus improving the numbers of EPCs potentially available for vasculogenesis and wound healing. However, despite the ability of hyperoxia to increase circulating EPCs, there was no significant increase in the numbers of EPCs homing to diabetic wounds in response to HBO treatment, confirming prior reports that recruitment of EPCs from circulation to peripheral tissue in diabetes is impaired. Thus, we hypothesized that unfavorable local wound conditions, such as decreased levels of the key EPC-homing chemokine, SDF-1α, may explain the diabetic EPC-homing defect and, hence, the disparity between circulating EPC numbers and wound-level EPCs in HBO-treated diabetic animals.

SDF-1α expression is decreased in diabetic peripheral cutaneous wounds. Physiologically, SDF-1α is one of the primary chemokines responsible for the mobilization and homing of EPCs to ischemic tissue (8, 15, 35). SDF-1α expression is known to be induced in a wide variety of cell types in response to stimuli such as stress and injury (36–38). The role of SDF-1α in diabetes-related chronic wounds has not been previously studied. Recent studies have indicated that in diabetes, the impaired neovascularization and delayed healing of cutaneous wounds is at least in part due to the reduced number and function of EPCs (28, 30, 39), but it is likely that other tissue-level factors contribute to poor wound healing in diabetes. To examine this issue, we investigated whether the diabetic phenotype is associated with decreased expression of SDF-1α in wound granulation tissue. Peripheral wound tissue from both diabetic and nondiabetic mice at various time points (days 5, 7, and 9 following STZ treatments) was harvested and examined using quantitative real-time RT-PCR. Our results demonstrate that *SDF-1α* decreased significantly (~50%) at day 9 following STZ treatments (Figure 3A). Moreover, fluorescent microscopy for cells expressing SDF-1 was performed on wounds 10 days after STZ treatment and 24 hours after creation of initial wound. Approximately half as many cells from diabetic wounds expressed SDF-1α as compared to wound cells from nondiabetic mice (Supplemental Figure 1; supplemental material available online with this article; doi:10.1172/JCI29710DS1). To identify the type(s) of cell(s) responsible for SDF-1α expression in diabetic wounds, a series of double-staining (SDF-1α and cell type–specific antigen) experiments were performed to examine myofibroblasts (α-SMC actin), epithelial cells (keratin 5), inflammatory cells (CD3/CD4), and ECs (CD31). Epithelial cells and myofibroblasts appeared to be responsible for the downregulation of SDF-1α in diabetic wounds (Figure 3B). Thus, in diabetic wounds, decreased expression of SDF-1α by epithelial cells and myofibroblasts may account for the lack of homing of EPCs to peripheral wounds, despite the increased systemic release of EPCs after HBO treatment. These findings suggest a novel therapeutic target that has not been previously studied in diabetic wound healing.

HBO and SDF-1α synergistically increase circulating EPCs in diabetic mice. Based on our findings that SDF-1α expression in peripheral tissue is decreased in diabetes, we set out to study the effects of exogenous administration of SDF-1α via local wound injections (both alone and in combination with HBO) on EPC mobilization, wound tissue homing, and wound healing in diabetic mice. We hypothesized a potential synergism on EPC tissue-level homing and wound healing using HBO and SDF-1α as combined thera-

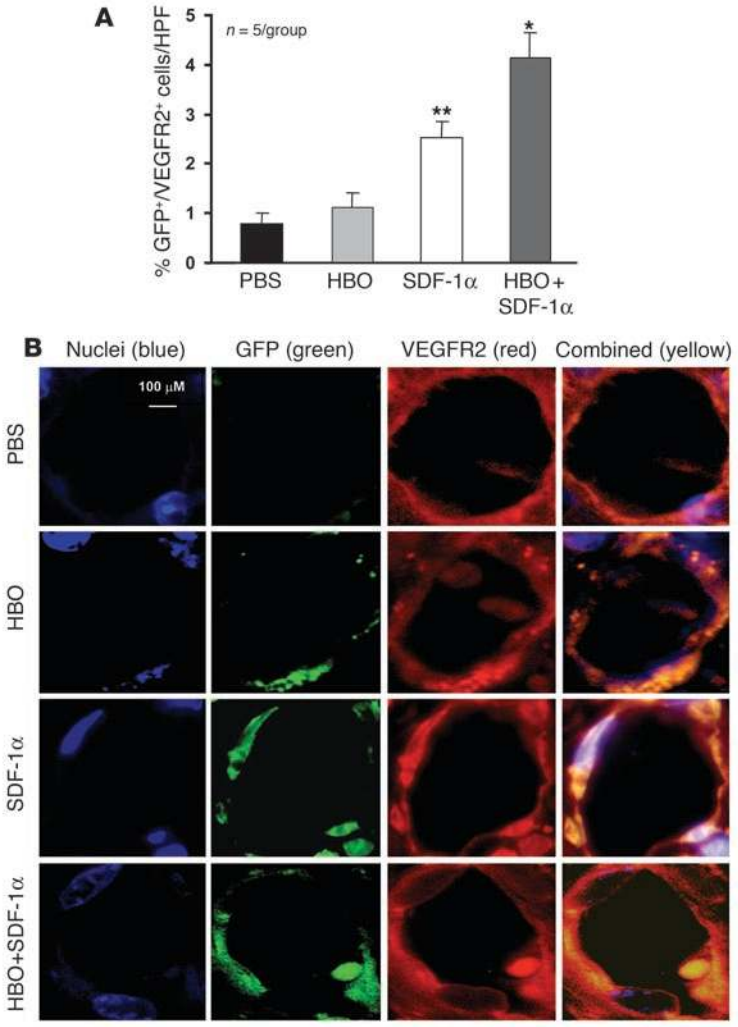

Figure 5
Impaired EPC homing to wound tissue in diabetes is reversed by cutaneous administration of SDF-1α. BM cells from GFP mice were transplanted into γ-irradiated FVB mice. Four groups of wounded diabetic chimeric mice were treated with daily wound injections of PBS, HBO, SDF-1α, or HBO+SDF-1α. After 3 days of treatment, wounds were harvested and analyzed by fluorescent immunostaining of tissue sections with anti–GFP-FITC or anti–VEGFR2-PE Abs. Nuclei were counterstained with Hoescht dye. Recruited EPCs were identified as $GFP^+/VEGFR2^+$ cells. (**A**) Quantification of recruited EPCs in diabetic mice. For each animal, 10 random high-power fields (HPFs, ×100) from 5 serial cross-sections were analyzed, and $GFP^+/VEGFR2^+$ cells were quantified relative to the total wound cellularity. Data are based on 3 experiments. SDF-1α+HBO–treated mice had a significant increase in the amount of recruited EPCs compared with other groups (*$P < 0.05$). SDF-1α–treated animals had a significant increase in amount of tissue EPCs compared with PBS control (**$P < 0.05$). HBO did not significantly enhance EPC homing to wounds. (**B**) Representative fluorescent immunostaining of wound sections are shown.

peutic strategies. Interestingly, we observed enhanced EPC mobilization in the SDF-1α + HBO–treated diabetic animals. We had specifically theorized that hyperoxia would enhance EPC mobilization while SDF-1α wound injections would increase homing to diabetic wounds and have a minimal impact on the number of circulating EPCs. Confirming our previous findings, tissue-level hyperoxia induced an increase in the mobilization of EPCs into circulation in wounded diabetic mice, as assessed by flow cytometry of the peripheral blood for cells coexpressing CXCR4 and VEGFR2 (Figure 4, A and B). In these mice, HBO treatment resulted in an approximately 4-fold increase in the percentage of circulating EPCs. Interestingly, local wound injections of SDF-1α resulted in a 2-fold increase in the number of EPCs in circulation. Perhaps most striking, the combination of HBO and peripheral wound SDF-1α administration resulted in a synergistic 11-fold increase in circulating EPCs. The mechanisms responsible for this dramatic synergistic enhancement in EPC mobilization in diabetic mice treated with HBO + SDF-1α require further study. We postulate that alteration of the cytokine milieu of the wound granulation tissue in favor of EPC homing and wound healing may lead to broad paracrine effects from factors released by the wound that, at a systemic level, further enhance BM EPC release. These local factors appear to work in synergism with hyperoxia to greatly increase the systemic mobilization of EPCs. Local wound injections with SDF-1α resulted in supraphysiologic levels of this chemokine within the diabetic wounds, as demonstrated by SDF-1α staining of the wound tissue in diabetic compared with baseline levels of the normal nondiabetic wounds (Figure 4C). In addition, the SDF-1α wound injections resulted in transient supra-physiologic levels of this chemokine within peripheral blood 2 hours (but not 24 hours; data not shown) after local injection (Figure 4D).

SDF-1α enhances EPC homing in diabetic peripheral cutaneous wounds. In order to determine the effect of SDF-1α on homing of the hyperoxia-mobilized EPCs to cutaneous wounds, we carried out BM transplantation experiments, wherein BM from GFP mice was transplanted into γ-irradiated FVB mice. After 3 weeks, chimeric mice were injected with STZ to induce diabetes. Once the mice were diabetic, wounds were created. Wounded diabetic chimeric mice were treated with both HBO, to mobilize EPCs into circulation, and local wound SDF-1α injections, to correct the observed decreased levels of this homing cytokine in diabetic wounds. We hypothesized that the combination of these 2 treatments, by addressing both central systemic release and peripheral homing of EPCs, would result in a synergistic enhancement of EPCs available for recruitment and participation in wound healing. The combination treatment was clearly superior to either modality

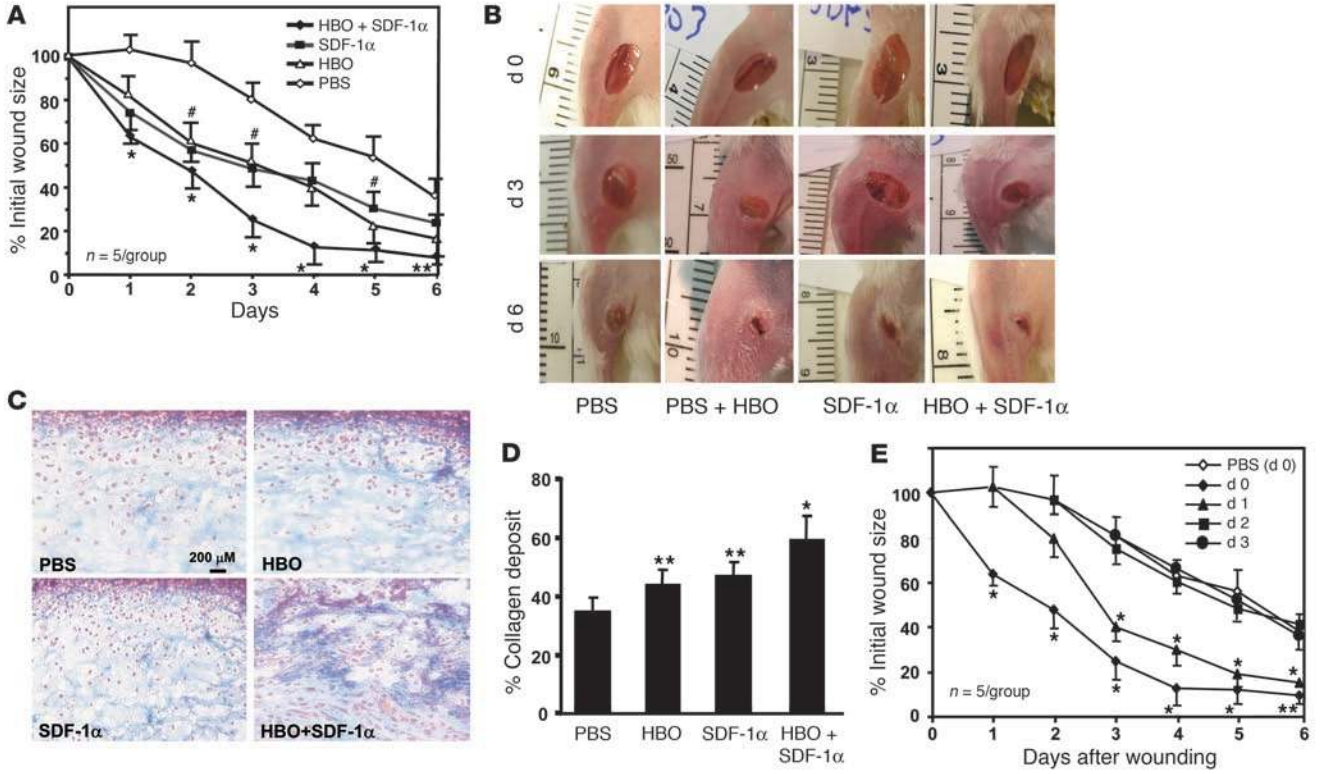

Figure 6

Synergistic effect of SDF-1α and HBO on diabetic wound healing. (**A**) Four groups of wounded diabetic mice were treated daily with PBS, HBO, SDF-1α, or HBO+SDF-1α. The fraction of initial wound size was measured daily by digital photography and analyzed with ImageJ for 6 days after wounding. Each point represents the mean of 5 experiments. Diabetic mice treated with SDF-1α+HBO had significantly improved wound healing rates at all time points when compared with PBS-treated controls (*$P < 0.001$ at days 1–5; **$P < 0.05$ at day 6). Diabetic mice treated with either HBO or SDF-1α demonstrated significantly improved wound healing over PBS controls at days 2, 3, and 5 (#$P < 0.05$). (**B**) Representative wounds at days 0, 3, and 6 are shown for each group. (**C**) Trichrome staining of wound tissues at day 6. Collagen was stained as blue. (**D**) Quantification of collagen content. Data are based on 5 scanned slides in each group at day 6. Data are based on 3 experiments. SDF-1α+HBO–treated mice demonstrated a significant rise in wound vessel density and collagen deposit compared with individual treatments alone (*$P < 0.05$), while SDF-1α and HBO treatments alone had significant increases compared with PBS control (**$P < 0.05$) at day 6. (**E**) Effect of timing in the initiation of SDF-1α+HBO therapy on wound healing in diabetic mice. Wound closure rates were monitored when treatment was started at days 0, 1, 3, and 5 after wounding and compared with the PBS treated group. Early treatment (days 0 and 1) was necessary to achieve increased closure rate.

alone, with HBO not significantly changing the number of EPCs ($GFP^+/VEGFR2^+$) present in wound tissue and SDF-1α resulting in a modest but significant 3-fold increase in the number of wound-level EPCs (Figure 5). A synergistic 5-fold increase in the number of EPCs was observed in wound tissue of diabetic mice treated with both HBO and SDF-1α compared with wound tissue of untreated diabetic mice. Similarly, a significantly increased number of $CXCR4^+/VEGFR2^+$ EPCs were observed in wound tissue of diabetic FVB mice (without BM transplantation) treated with both HBO and SDF-1α as compared with wound tissue of untreated control mice ($P < 0.05$; Supplemental Figure 2). Our data indicate that multi-modality therapy aimed at improving both mobilization and homing of EPCs is an effective strategy to have a significant impact on the number of EPCs available in wound tissue.

The combination of hyperoxia and SDF-1α significantly enhances wound healing in diabetic mice. EPCs play a key role in vasculogenesis and cutaneous tissue repair (6, 40). We hypothesized that increased numbers of EPCs in circulation, along with enhanced EPC homing to wounds, results in improved wound healing in diabetes. We studied diabetic wound closure rates in response to treatment with HBO and SDF-1α alone and in combination. Wounded diabetic mice underwent daily wound injections with SDF-1α, PBS, HBO, or SDF-1α + HBO treatments. Only 3 days after initial injury, wound area was found to decrease by 75% in the group treated with SDF-1α + HBO, as compared with a 20% decrease in the PBS controls (Figure 6, A and B). This healing response was greater than the response to either treatment modality alone. In addition, histochemical analysis was conducted to examine blood vessel density (VEGFR2 staining), cellularity and stromagenesis (H&E staining), and extracellular constitution (trichrome staining) in wound tissues. Compared with treatment with either HBO or SDF-1α, combined HBO + SDF-1α therapy substantially promoted angiogenesis and stromagenesis (Supplemental Figure 3) and the deposition of collagen in the granulation tissue (Figure 6, C and D). These data provide substantial evidence to support the synergistic effect of HBO + SDF-1α therapy on accelerating diabetic wound healing. Overall, our data support the conclusion that these therapies used in concert result in accelerated cutaneous wound healing in diabetic mice. To determine the effect of timing in the initiation of HBO + SDF-1α therapy on wound healing in diabetic

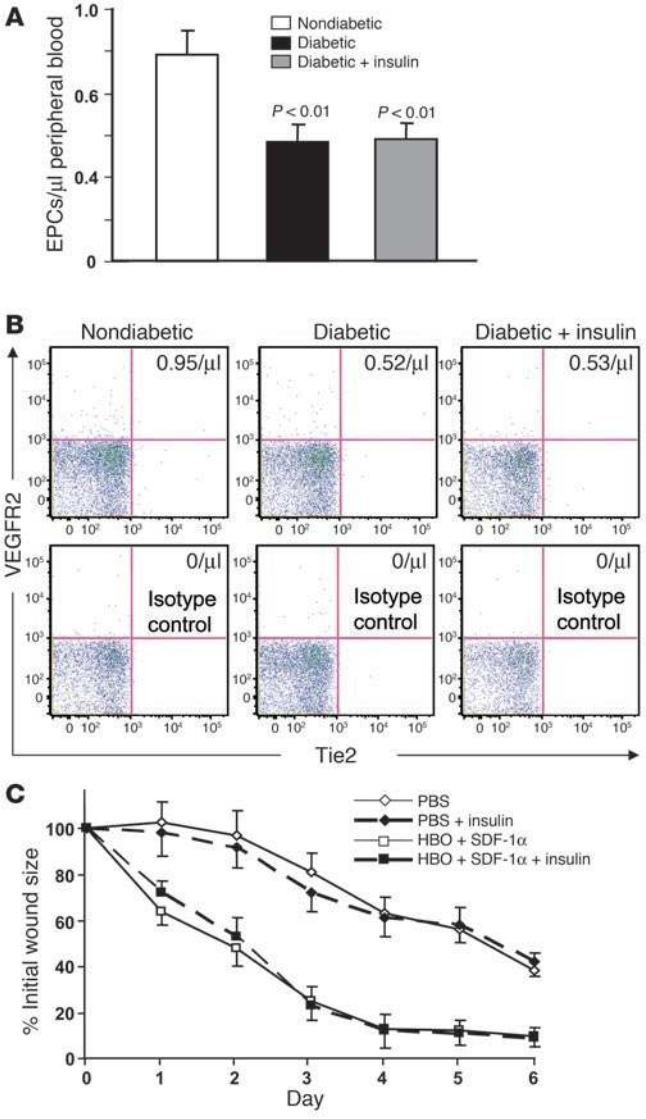

Figure 7
Insulin does not increase EPC mobilization or wound healing in diabetic mice. (**A**) Quantification of circulating EPCs by flow cytometry. Data are based on 3 experiments. (**B**) Representative dot plots are shown, with number of peripheral blood EPCs noted in each of the $VEGFR2^+/Tie2^+$ quadrants. (**C**) Minimal effect of insulin on wound healing rate in PBS- or HBO+SDF-1α–treated diabetic mice ($n = 10$ in each group). Data are based on 2 experiments. No statistical significance was observed in wound closure rates when insulin was introduced to achieve euglycemia.

mice, we examined wound closure rates when HBO + SDF-1α treatment was initiated on days 0, 1, 3, and 5 following wounding. Our results show that in order to influence wound healing, early application of HBO + SDF-1α is necessary, as initiation of treatment either at initial wounding or 1 day after wounding is effective, while delayed treatment (day 3 or 5) results in the loss of accelerated wound closure rates (Figure 6E).

Insulin is insufficient to restore impaired diabetic wound healing. As insulin is a standard therapy for type I diabetes, we examined the effects of insulin on impaired eNOS/NO/EPC mobilization/wound healing in diabetic mice. STZ-induced diabetic mice were treated with insulin (6 U/kg NPH [isophane] insulin i.p. twice per day) for the duration of each experiment. The mice with therapeutic euglycemia (glucose <200 mg/dl) were then utilized in these experiments. Interestingly, insulin alone had little effect in reversing impaired BM eNOS phosphorylation (Figure 1A), BM NO production (Figure 1D), or EPC mobilization (Figure 7, A and B) in diabetic mice. Similarly, insulin treatment failed to improve impaired wound SDF-1α production (data not shown) and wound healing rates (Figure 7C). When combined with HBO + SDF-1α therapy, insulin treatment did not further accelerate the wound healing rate. Our data indicate that short-term insulin treatment has minimal effects on improving diabetic wound healing.

Discussion

The mechanisms responsible for decreased circulating and wound level EPCs in diabetes have not been previously determined (28–30). This study addressed this fundamental question. Here we show that phosphorylation of eNOS in BM is impaired and that SDF-1α expression by epithelial cells and myofibroblasts in the granulation tissue of cutaneous wounds is decreased in this diabetic murine model. Impaired phosphorylation of eNOS in the BM and decreased wound expression of SDF-1α have a direct impact on EPC mobilization from BM into circulation and EPC homing to wounds, respectively, and can be therapeutically reversed to enhance EPCs available in peripheral wound tissue and improve wound healing. By utilizing HBO to induce tissue-level hyperoxia, we have shown that multiple BM NOS isoforms may be activated, leading to increased NO levels in the BM and hence enhanced mobilization of EPCs into the circulation, thus partially reversing the defect in eNOS activation and EPC release caused by diabetes. In addition, by increasing wound levels of SDF-1α, we have shown that not only is the diabetic EPC homing impairment reversed, but also a synergistic increase in EPC mobilization, homing, and wound healing may be achieved when used in conjunction with HBO. The novel targets identified by this study (HBO-mediated EPC release by NOS activation and SDF-1α–mediated EPC homing), along with knowledge about the timing for the initiation of these therapies, carry important clinical relevance for advancement in the field of diabetic wound healing. These data provide the foundation for significant improvements on existing clinical protocols for this significant unsolved medical problem.

Our findings are consistent with prior reports showing that hyperglycemia and diabetes mellitus are associated with impaired eNOS function in a variety of tissues (18, 20, 41). Specifically, hyperglycemia has been found to inhibit eNOS phosphorylation in bovine arterial ECs in vitro by posttranslational modification at the Akt site (18). Furthermore, insulin resistance has been shown to impair eNOS activity by increasing endothelial fatty acid oxidation, a potential mechanism whereby diabetes mellitus results in accelerated atherogenesis and increased cardiovascular disease risk (20). Therefore, our finding that eNOS phosphorylation is impaired in diabetic BM, resulting in depressed EPC mobilization into circulation, builds on recent findings detailing eNOS dysfunction in vitro and in other physiologic systems in diabetic patients (41). In addition, our studies show the inability of insulin treatment to reverse impaired BM eNOS phosphorylation, NO production, EPC mobilization, and wound healing in diabetic mice. This is not surprising, as our results only reflect the short-term effect of

insulin on diabetic wound healing. The effects of long-term treatment with insulin on chronic wound healing in diabetes remain to be studied.

Our data suggest that hyperoxia activates NOS in the BM, thus inducing EPC mobilization into circulation by increasing BM NO production. In diabetic mice, the hyperoxia-induced increase in BM NO was attenuated, likely as a result of impaired eNOS phosphorylation. However, with the induction of hyperoxic conditions, other NOS isoenzymes appear to compensate, leading to NO increases in the BM that are substantial and sufficient to reverse the defect in EPC mobilization in our diabetic mouse model.

Although G-CSF and other chemokines have been shown to increase circulating EPCs (42), there is an associated increase in leukocytes resulting in inflammation with the potential for enhanced acute coronary events, which raises questions about the safety and clinical utility of these chemokines (43, 44). This study shows that in the setting of diabetes, hyperoxia increases BM NO levels and stimulates EPC release from the BM into circulation without having a significant impact on the inflammatory cell numbers in circulation. Given that the reduced number of peripheral EPCs is an important contributor to the poor neovascularization and wound healing in diabetic patients, the potential to exploit this mechanism for therapeutic use becomes inherent.

Hyperoxia appears to involve a signal cascade similar to the sequence of events detailing hypoxia-induced EPC release (6–9, 11, 13, 15). The reasons for this seemingly paradoxical response to hyperoxia are unclear, but based on our findings and the reported effects of hypoxia, both hypoxia and hyperoxia result in NOS activation and a subsequent increase in BM NO level. One possible explanation for this response involves the possibility that an oxygen tension sensor, triggered by any perturbation in the oxygen levels, results in NO production and EPC release. Another potential explanation is that both high and low local oxygen concentrations act via distinct mechanisms that ultimately converge on NOS activation. Whatever the reason, it is clear that with hypoxia, systemic effects of VEGF-A via VEGFR2 mediate NOS activation, whereas with hyperoxia, NO levels rise within minutes and the effects are quickly reversible upon withdrawal of the stimulus, suggesting a direct activation of NOS by a change in oxygen tension. Further studies are needed to more specifically examine this question.

Our data demonstrate that hyperoxia selectively enhances EPC release, resulting in a small but significant improvement in diabetic wound healing but not having a significant impact on wound EPC homing. This may explain the variable clinical effects on wound healing reported with HBO treatment alone. We postulate that the HBO-mediated enhancement of wound healing is multifactorial. Likely there are systemic paracrine effects due to increased circulating EPCs that in some circumstances may be sufficient to modestly enhance wound healing. In addition, HBO may have local tissue effects unrelated to EPC release that also enhance wound healing in selective wound environments. One of these effects may include increased tissue-level release of angiogenic factors such as VEGF-A (45, 46). We were interested in investigating potential factors that may work in conjunction with hyperoxia to promote recruitment of EPCs and wound repair in the setting of diabetes. Specifically, we examined the role of SDF-1α in diabetic wounds. While it is known that SDF-1α is the predominant chemokine that is upregulated in ischemic tissue and acts as a homing signal for EPCs (15, 35, 47), the effect of SDF-1α expression at the tissue level in diabetes had not been previously studied, and our findings represent what we believe to be the first report on the important role of SDF-1α in diabetic wound healing. Strategies for EPC mobilization are only clinically relevant if the results affect tissue neovascularization and wound healing. If EPCs are mobilized into circulation but fail to reach the injured tissue, the clinical usefulness of the treatment becomes questionable. Previous literature has focused on either improving mobilization of EPCs or enhancing EPC homing to ischemic tissue, but strategies for mobilization in combination with homing to optimize recruitment of these cells to diabetic wounds have not been previously studied, as mechanism-oriented rationales for testing these new hypotheses were lacking. Our findings provide the preclinical rational for further studies targeting BM eNOS activation, activation of other BM NOS isoenzymes, and tissue-level SDF-1α expression to enhance EPC mobilization, homing, and wound healing in diabetes.

Methods

Mice. All procedures were done with approval from the University of Pennsylvania Institutional Animal Care and Use Committee. Six- to twelve-week-old FVB wild-type (FVB/NJ), GFP (FVB/Tg), Tie2-GFP [Tg(TIE2GFP)87 Sato/J] (48, 49), and eNOS$^{-/-}$ (B6.129P2-*Nos3*^{tm1Unc}/J) mice were purchased from The Jackson Laboratory. For all surgical procedures, mice were anesthetized with an i.p. injection of 80 mg/kg of ketamine (Phoenix Scientific Inc.) and 20 mg/kg xylazine (Vedco Inc.). For BM transplantation experiments, 1×10^7 BM cells from GFP mice were transplanted into γ-irradiated (900 Rad) FVB wild-type mice via tail vein. Reconstitution of transplanted BM in chimeras was achieved at 3 weeks and confirmed by FACScan (>50% BM cells were GFP$^+$; data not shown). For local wound SDF-1α injection, SDF-1α protein (R&D Systems) was reconstituted in PBS and injected into the wound base (25 μg/kg).

Induction of diabetes and generation of peripheral wounds. Tie2-GFP and wild-type or chimeric FVB mice at 6–12 weeks of age were treated with STZ (Sigma-Aldrich) to induce diabetes. Mice were rendered diabetic by i.p. administration of 60 mg/kg STZ in 50 mM sodium citrate, pH 4.5, daily for 5 days (50). Control mice were treated with daily injections of citrate buffer. Serum glucose was measured from the mouse tail vein using a glucometer. Once serum glucose reached 250 mg/dl, mice were followed with daily measurements for 1 week prior to use in experiments. Mean serum glucose levels in STZ mice 461 mg/dl with a range of 372–520 mg/dl, while mean control mouse serum glucose levels were 120 mg/dl with a range of 94–135 mg/dl. Wounds were induced on the ventral surface of the mouse thigh using a 4-mm punch biopsy. Full-thickness skin was removed, exposing the underlying muscle.

HBO treatment and in vivo BM NO measurements. For HBO treatment, mice were placed in an animal hyperbaric chamber (Reneau Inc.) and subjected to 100% oxygen at 2.4 atmosphere absolute for 90 minutes (51). To measure continuous real-time BM NO levels, Nafion (Sigma-Aldrich) polymer-coated NO microelectrodes (21, 52, 53) were inserted into the femoral BM cavity as previously described (23). An osteotomy was created on the patellar surface of the murine femur using a 25G beveled needle, allowing the electrode to be lowered into the BM space when the animal was placed in the hyperbaric chamber. In some mice, pretreatment with L-NAME (40 mg/kg i.p.) (Sigma-Aldrich) was given 2 hours prior to exposure to HBO.

Western blot analysis. Whole BM was isolated from FVB/NJ mice (n = 12/group) by flushing harvested femurs and tibias with PBS/2% FBS. Red blood cells were removed by Red Cell Lysis Buffer (Sigma-Aldrich). Isolated BM cells were then lysed, and protein concentrations were determined by DC protein assay (Bio-Rad). Equal amounts of protein were subjected to 4%–12% SDS gel electrophoresis under reducing conditions. The transferred PVDF membranes were probed with primary Ab (anti-eNOS, anti–phospho-

eNOS [Ser^{1177}], anti-iNOS, and anti-nNOS; BD Biosciences) diluted 1:500 in 1% milk in Tris-buffered saline with Tween buffer and then incubated with HRP-conjugated secondary Ab (DakoCytomation). Proteins were visualized using enhanced chemiluminescence (ECL kit; Amersham Biosciences).

Real-time RT-PCR. Total RNA was isolated from wound tissues using TRIzol reagents (Invitrogen) in tissue grinders. cDNA was synthesized from 500 ng of total RNA using TaqMan Gold RT-PCR Kit (Applied Biosystems) according to the manufacturer's protocol. The cDNA samples were diluted 20-fold, and real-time PCR reaction was carried out using SYBR Green JumpStart Taq ReadyMix (Sigma-Aldrich) with 100 μM of primer. Amplifications were performed in an ABI PRISM 7000 Sequence Detection System (Applied Biosystems). Thermal cycler conditions were 50°C for 2 minutes and 95°C for 10 minutes to activate or inactivate various enzymes, then 40 cycles each of 15 seconds at 95°C (denaturation) followed by 1 minute at 59°C (annealing and extension). The β-actin plasmid was used as standard DNA. All standards and samples were assayed in triplicate. The threshold cycle values were used to plot a standard curve. All samples were normalized to the relative levels of β-*actin* (which was set as "1"), and results were expressed as fold-increase. Primers were designed using Primer Express software (version 2.0; Applied Biosystems) as follows: *SDF-1*α, 5′-CCAGAGCCAACGTCAAGCAT-3′ and 5′-TGTTGAGGATTTTCAGATGCTTGA-3′; β-*actin*, 5′-ACGGCCAGGTCATCACTATTG-3′ and 5′-CAAGAAGGAAGGCTGGAAAAGA-3′.

ELISA. Mouse serum SDF-1α concentration was measured by Quantikine mouse SDF-1α ELISA kit (R&D Systems) based on the manufacturer's protocol.

Flow cytometry. Mobilization of EPCs into circulation was studied using flow cytometry as previously described (23). Cells isolated from mice were incubated with various Abs (BD Biosciences). Isotype-matched mouse immunoglobulins served as controls. One million viable cells were scanned, and lymphocytes were gated and analyzed using an LSR II multicolor flow cytometer (BD Biosciences). Data was analyzed using FlowJo software (version 6.4.3; Treestar Inc.).

Histochemistry. For immunostaining, paraffin-embedded serial sections (5 μm) first underwent standard deparaffinization and rehydration procedures and were then probed with various Abs. To assess wound SDF-1α$^+$ cells, sections were double stained with FITC-conjugated anti–SDF-1α and PE-conjugated tissue-specific Abs (eBiosciences). To detect the blood vessels in wounds, sections were stained with FITC-conjugated anti-VEGFR2 Ab. For examination of wound EPC recruitment in the BM transplantation experiment, sections were double stained with FITC-GFP and PE-VEGFR2 (BD Biosciences). Nuclei were counterstained with Hoescht dye. Masson's trichrome staining and H&E staining were performed using standard methods, and all reagents were from Sigma-Aldrich. Tissue sections were analyzed using fluorescence microscopy and ImageJ software (version 6.0; NIH) to quantitate fluorescent intensity. In trichrome-stained slides, blue stain (collagen content) was also quantitatively analyzed using ImageJ.

Assessment of peripheral wound healing. Initial wound surface area was recorded, and the healing of wounds was recorded daily with digital photographs with daily digital photographs using an Olympus digital camera. Photographs contained an internal scale to allow for standard calibration of measurements. Wound area was quantified using ImageJ software and was expressed as the percentage of original wound size. Wounds were observed for 6 days, and mice were sacrificed at the conclusion of the experiment.

Statistics. All data is expressed as mean ± SEM. Statistical analysis was carried out using paired 2-tailed Student's *t* test and ANOVA procedures. $P < 0.05$ was considered statistically significant.

Acknowledgments

This work was supported by NIH grants 1-R01-DK071084 and K-01-HL073145 and by University of Pennsylvania Institutional Research Funds.

Received for publication July 14, 2006, and accepted in revised form February 6, 2007.

Address correspondence to: Omaida C. Velazquez, Department of Surgery, University of Pennsylvania Medical Center, 4th floor Silverstein Pavilion, 3400 Spruce Street, Philadelphia, Pennsylvania 19104-4283, USA. Phone: (215) 662-6451; Fax: (215) 662-4871; E-mail: omaida.velazquez@uphs.upenn.edu.

Katherine A. Gallagher and Zhao-Jun Liu contributed equally to this work.

1. Centers for Disease Control and Prevention. 1998. Diabetes-related amputations of lower extremities in the Medicare population — Minnesota, 1993–1995. *MMWR Morb. Mortal. Wkly. Rep.* **47**:649–652.
2. Feener, E.P., and King, G.L. 1997. Vascular dysfunction in diabetes mellitus. *Lancet.* **350**(Suppl. 1):SI9–SI13.
3. Phillips, T.J. 1994. Chronic cutaneous ulcers: etiology and epidemiology. *J. Invest. Dermatol.* **102**:38S–41S.
4. Hanahan, D. 1997. Signaling vascular morphogenesis and maintenance. *Science.* **277**:48–50.
5. Carmeliet, P. 2000. Developmental biology. One cell, two fates. *Nature.* **408**:43, 45.
6. Tepper, O.M., et al. 2005. Adult vasculogenesis occurs through in situ recruitment, proliferation, and tubulization of circulating bone marrow–derived cells. *Blood.* **105**:1068–1077.
7. Rafii, S., and Lyden, D. 2003. Therapeutic stem and progenitor cell transplantation for organ vascularization and regeneration. *Nat. Med.* **9**:702–712.
8. Yamaguchi, J., et al. 2003. Stromal cell–derived factor-1 effects on ex vivo expanded endothelial progenitor cell recruitment for ischemic neovascularization. *Circulation.* **107**:1322–1328.
9. Asahara, T., et al. 1997. Isolation of putative progenitor endothelial cells for angiogenesis. *Science.* **275**:964–967.
10. Kawamoto, A., et al. 2001. Therapeutic potential of ex vivo expanded endothelial progenitor cells for myocardial ischemia. *Circulation.* **103**:634–637.
11. Takahashi, T., et al. 1999. Ischemia- and cytokine-induced mobilization of bone marrow–derived endothelial progenitor cells for neovascularization. *Nat. Med.* **5**:434–438.
12. Gill, M., et al. 2001. Vascular trauma induces rapid but transient mobilization of VEGFR2(+)AC133(+) endothelial precursor cells. *Circ. Res.* **88**:167–174.
13. Aicher, A., et al. 2003. Essential role of endothelial nitric oxide synthase for mobilization of stem and progenitor cells. *Nat. Med.* **9**:1370–1376.
14. Murohara, T., et al. 1998. Nitric oxide synthase modulates angiogenesis in response to tissue ischemia. *J. Clin. Invest.* **101**:2567–2578.
15. Ceradini, D.J., et al. 2004. Progenitor cell trafficking is regulated by hypoxic gradients through HIF-1 induction of SDF-1. *Nat. Med.* **10**:858–864.
16. Bivalacqua, T.J., et al. 2004. RhoA/Rho-kinase suppresses endothelial nitric oxide synthase in the penis: a mechanism for diabetes-associated erectile dysfunction. *Proc. Natl. Acad. Sci. U. S. A.* **101**:9121–9126.
17. Bucci, M., et al. 2004. Diabetic mouse angiopathy is linked to progressive sympathetic receptor deletion coupled to an enhanced caveolin-1 expression. *Arterioscler. Thromb. Vasc. Biol.* **24**:721–726.
18. Du, X.L., et al. 2001. Hyperglycemia inhibits endothelial nitric oxide synthase activity by post-translational modification at the Akt site. *J. Clin. Invest.* **108**:1341–1348. doi:10.1172/JCI200111235.
19. Szabo, C., et al. 2002. Poly(ADP-ribose) polymerase is activated in subjects at risk of developing type 2 diabetes and is associated with impaired vascular reactivity. *Circulation.* **106**:2680–2686.
20. Du, X., et al. 2006. Insulin resistance reduces arterial prostacyclin synthase and eNOS activities by increasing endothelial fatty acid oxidation. *J. Clin. Invest.* **116**:1071–1080. doi:10.1172/JCI23354.
21. Thom, S.R., et al. 2002. Stimulation of nitric oxide synthase in cerebral cortex due to elevated partial pressures of oxygen: an oxidative stress response. *J. Neurobiol.* **51**:85–100.
22. Thom, S.R., et al. 2003. Stimulation of perivascular nitric oxide synthesis by oxygen. *Am. J. Physiol. Heart Circ. Physiol.* **284**:H1230–H1239.
23. Goldstein, L.J., et al. 2006. Endothelial progenitor cell release into circulation is triggered by hyperoxia-induced increases in bone marrow nitric oxide. *Stem Cells.* **24**:2309–2318.
24. Kessler, L., et al. 2003. Hyperbaric oxygenation accelerates the healing rate of nonischemic chronic diabetic foot ulcers: a prospective randomized study. *Diabetes Care.* **26**:2378–2382.
25. Kranke, P., Bennett, M., Roeckl-Wiedmann, I., and Debus, S. 2004. Hyperbaric oxygen therapy for chronic wounds. *Cochrane Database Syst. Rev.* **2**:CD004123.
26. Abidia, A., et al. 2003. The role of hyperbaric oxy-

gen therapy in ischaemic diabetic lower extremity ulcers: a double-blind randomised-controlled trial. *Eur. J. Vasc. Endovasc. Surg.* **25**:513–518.
27. Fedyk, E.R., Ryyan, D.H., Ritterman, I., and Springer, T.A. 1999. Maturation decreases responsiveness of human bone marrow B lineage cells to stromal-derived factor 1 (SDF-1). *J. Leukoc. Biol.* **66**:667–673.
28. Tepper, O.M., et al. 2002. Human endothelial progenitor cells from type II diabetics exhibit impaired proliferation, adhesion, and incorporation into vascular structures. *Circulation.* **106**:2781–2786.
29. Vasa, M., et al. 2001. Number and migratory activity of circulating endothelial progenitor cells inversely correlate with risk factors for coronary artery disease. *Circ. Res.* **89**:E1–E7.
30. Fadini, G.P., et al. 2005. Circulating endothelial progenitor cells are reduced in peripheral vascular complications of type 2 diabetes mellitus. *J. Am. Coll. Cardiol.* **45**:1449–1457.
31. Rafii, S., et al. 2003. Angiogenic factors reconstitute hematopoiesis by recruiting stem cells from bone marrow microenvironment. *Ann. N. Y. Acad. Sci.* **996**:49–60.
32. Llevadot, J., et al. 2001. HMG-CoA reductase inhibitor mobilizes bone marrow–derived endothelial progenitor cells. *J. Clin. Invest.* **108**:399–405. doi:10.1172/JCI200113131.
33. Verma, S., et al. 2004. C-reactive protein attenuates endothelial progenitor cell survival, differentiation, and function: further evidence of a mechanistic link between C-reactive protein and cardiovascular disease. *Circulation.* **109**:2058–2067.
34. Mohle, R., Rafii, S., and Moore, M.A. 1998. The role of endothelium in the regulation of hematopoietic stem cell migration. *Stem Cells.* **16**(Suppl. 1):159–165.
35. Peled, A., et al. 1999. The chemokine SDF-1 stimulates integrin-mediated arrest of $CD34^+$ cells on vascular endothelium under shear flow. *J. Clin. Invest.* **104**:1199–1211.
36. Lee, R.H., et al. 2006. A subset of human rapidly self-renewing marrow stromal cells preferentially engraft in mice. *Blood.* **107**:2153–2161.
37. Miller, J.T., et al. 2005. The neuroblast and angioblast chemotaxic factor SDF-1 (CXCL12) expression is briefly up regulated by reactive astrocytes in brain following neonatal hypoxic-ischemic injury. *BMC Neurosci.* **6**:63.
38. Urbich, C., et al. 2005. Soluble factors released by endothelial progenitor cells promote migration of endothelial cells and cardiac resident progenitor cells. *J. Mol. Cell. Cardiol.* **39**:733–742.
39. Keswani, S.G., et al. 2004. Adenoviral mediated gene transfer of PDGF-B enhances wound healing in type I and type II diabetic wounds. *Wound Repair Regen.* **12**:497–504.
40. Bauer, S.M., et al. 2006. The bone marrow–derived endothelial progenitor cell response is impaired in delayed wound healing from ischemia. *J. Vasc. Surg.* **43**:134–141.
41. Musicki, B., Kramer, M.F., Becker, R.E., and Burnett, A.L. 2005. Inactivation of phosphorylated endothelial nitric oxide synthase (Ser-1177) by O-GlcNAc in diabetes-associated erectile dysfunction. *Proc. Natl. Acad. Sci. U. S. A.* **102**:11870–11875.
42. Powell, T.M., et al. 2005. Granulocyte colony-stimulating factor mobilizes functional endothelial progenitor cells in patients with coronary artery disease. *Arterioscler. Thromb. Vasc. Biol.* **25**:296–301.
43. Kang, H.J., et al. 2004. Effects of intracoronary infusion of peripheral blood stem-cells mobilised with granulocyte-colony stimulating factor on left ventricular systolic function and restenosis after coronary stenting in myocardial infarction: the MAGIC cell randomised clinical trial. *Lancet.* **363**:751–756.
44. Morimoto, A., Sakata, Y., Watanabe, T., and Murakami, N. 1990. Leucocytosis induced in rabbits by intravenous or central injection of granulocyte colony stimulating factor. *J. Physiol.* **426**:117–126.
45. Sheikh, A.Y., et al. 2000. Effect of hyperoxia on vascular endothelial growth factor levels in a wound model. *Arch. Surg.* **135**:1293–1297.
46. Sen, C.K., et al. 2002. Oxygen, oxidants, and antioxidants in wound healing: an emerging paradigm. *Ann. N. Y. Acad. Sci.* **957**:239–249.
47. Peled, A., et al. 1999. Dependence of human stem cell engraftment and repopulation of NOD/SCID mice on CXCR4. *Science.* **283**:845–848.
48. Sato, T.N., Qin, Y., Kozak, C.A., and Audus, K.L. 1993. Tie-1 and tie-2 define another class of putative receptor tyrosine kinase genes expressed in early embryonic vascular system. *Proc. Natl. Acad. Sci. U. S. A.* **90**:9355–9358.
49. Schlaeger, T.M., et al. 1997. Uniform vascular-endothelial-cell–specific gene expression in both embryonic and adult transgenic mice. *Proc. Natl. Acad. Sci. U. S. A.* **94**:3058–3063.
50. Park, L., et al. 1998. Suppression of accelerated diabetic atherosclerosis by the soluble receptor for advanced glycation endproducts. *Nat. Med.* **4**:1025–1031.
51. Sheffield, P.J. 2004. How the Davis 2.36 ATA wound healing enhancement treatment table was established. *Undersea Hyperb. Med.* **31**:193–194.
52. Buerk, D.G., Atochin, D.N., and Riva, C.E. 1998. Simultaneous tissue PO2, nitric oxide, and laser Doppler blood flow measurements during neuronal activation of optic nerve. *Adv. Exp. Med. Biol.* **454**:159–164.
53. Kashiwagi, S., et al. 2005. NO mediates mural cell recruitment and vessel morphogenesis in murine melanomas and tissue-engineered blood vessels. *J. Clin. Invest.* **115**:1816–1827. doi:10.1172/JCI24015.